doi: 10.1038/nature07174

Significant contribution of Archaea to extant biomass in marine subsurface sediments

Julius S. Lipp[1], Yuki Morono[2], Fumio Inagaki[2], and Kai-Uwe Hinrichs[1]

[1]*Organic Geochemistry Group, Department of Geosciences and MARUM Center for Marine Environmental Sciences, University of Bremen, PO Box 330 440, 28334 Bremen, Germany*

[2]*Geomicrobiology Group, Kochi Institute for Core Sample Research, Japan Agency for Marine-Earth Science and Technology (JAMSTEC), Monobe B200, Nankoku, Kochi 783-8502, Japan*

I. Materials and Methods

Sample collection

Samples were collected during ODP legs 201 (Peru margin and Eastern Equatorial Pacific), 204 (Hydrate ridge), 207 (Demerara rise), IODP expeditions 301 (Juan de Fuca Ridge flank) and 311 (Cascadia margin), *DV Chikyu* Shakedown Expedition CK06-06 (offshore the Shimokita Peninsula, Japan), Sonne cruise SO147 (Peru margin), Professor Logatchev cruise TTR15 (Black Sea), and Kaiyo cruise KY04-11 (Nankai trough). The sediments were immediately frozen and stored at -80 °C until extraction of lipids and DNA. Coupled sediments for analysis of both lipids and DNA were taken from core sections according to ODP/IODP standard sampling protocols with a difference in core depth of 0.5 to 1 m.

Extraction of intact polar lipids

Frozen material (10 - 50 g of wet sediment for ODP/IODP samples; 1-10 g of freeze-dried sediment for SO147, TTR15, KY04-11 samples) was spiked with an internal standard (1-O-hexadecyl-2-acetoyl-*sn*-glycero-3-phosphocholine; PAF) and extracted using a modified Bligh and Dyer protocol in four steps[1]. After centrifugation at 800 x g the supernatants were combined, washed with water and carefully evaporated to dryness under a stream of nitrogen at 35 °C and stored at -20 °C until analysis. Standard recovery was tested by spiking 5 g of sediment of two sediment samples (1225A-198.1 and 1227D-1.15) with an IPL mixture consisting of dipalmitoyl phosphatidylglycerol (di-C_{16}-PG), dipalmitoyl phosphatidyl-ethanolamine (di-C_{16}-PE), dipalmitoyl phosphatidylcholine (di-C_{16}-PC), and monoglycosyl glycerol dibiphytanyl glycerol tetraether phosphatidylglycerol (1-Gly-GDGT-PG) (see *Supplementary Figure 2*). Sediments were extracted according to the extraction protocol described above and standard recovery was calculated relative to a direct injection of the pure standard mixture. Extraction and analysis was done in duplicate and error bars were calculated according to error propagation from repeated analyses. Ion suppression (e.g. *ref. 2*) was monitored in a third experiment by mixing IPL standards with total lipid extract from sample 1227D-21.9, mimicking typical analytical conditions.

HPLC-MS analysis and quantification of IPLs

The total lipid extract was dissolved in 0.1 – 1 ml of methanol:DCM (1:1, v/v) and separated on a ThermoFinnigan Surveyor HPLC System equipped with a diol column coupled to a ThermoFinnigan LCQ Deca XP Plus ion trap mass spectrometer using an electrospray ionisation (ESI) ion source. Details of chromatography and mass spectrometry are provided in Sturt *et al.*[1]

Individual response factors relative to the internal standard PAF were determined by injection of a series of standard solutions (di-C16-PC, di-C16-PG, di-C16-PE, 1-Gly-DG, 1-Gly-GDGT-PG; Matreya, USA; Avanti Polar Lipids, USA) in amounts ranging from 1 ng to 500 ng. Absolute IPL concentrations were calculated from peak areas of molecular ions in mass chromatograms relative to PAF, taking the response factors of archaeal and bacterial IPLs in relation to the internal standard into account. Multiple extractions of different sediment aliquots from 10-cm subcores and repeated injection of the total lipid extract provided standard deviations (typically ~20%) of the absolute IPL concentrations for a subset of 31 samples. For samples in which exclusively archaeal IPLs were detected, the proportion of bacterial lipids was assumed to be the level of detection (LOD). The LOD was calculated in a similar manner to the absolute IPL concentrations from the minimum peak area that could be identified as a signal in the respective mass chromatograms (typically 10^8 peak area units). It was then corrected with the average response factor for the two standards di-C16-PG and di-C16-PE representing the most common bacterial IPL types and multiplied by a factor of two assuming that the diversity of bacterial IPLs is higher than the diversity of archaeal lipids due to the larger variation in carbon atom numbers of ester-bound fatty acids (i.e., in a typical sediment sample containing both archaeal and bacterial IPLs, typically twice as many individual bacterial compounds are identifiable). A signal-to-noise ratio (SNR) of higher than three was maintained for all analyses. All IPL concentrations were normalised to the volume of extracted sediment. The volume was calculated from the bulk density and mass of extracted sediment.

Preparation and analysis of phospholipid derived fatty acids (PLFA)

Total lipid extracts were fractionated on a glass column packed with 500 mg silica (Silica Gel 60, 60 - 200 µm, Roth, Germany) following the procedure of Mills *et al.*[3] The apolar fraction was eluted with 5 ml dichloromethane and the polar fraction with 10 ml acetone followed by 5 ml methanol. After evaporation to dryness, the polar fraction was dissolved in 1 ml of toluene/methanol (1:1, v/v) and subjected to mild alkaline methanolysis[4,5] to produce fatty acid methyl esters (FAMEs). FAMEs were dissolved in hexane and cholestane was added as injection standard. The identification and quantification was done on a Trace GC-MS system (ThermoFinnigan, San Jose, CA). The GC injector temperature was 310 °C in split/splitless mode and separation was achieved on a Restek Rxi-5ms capillary column (L=30 m; ID=0.25 mm; 0.25 µm film thickness; carrier gas: He at 1 ml/min flow rate). The GC was programmed to 60 °C (hold for 1 min), followed by heating at 10 °C/min to 150 °C, then 4°C/min to 320 °C (hold for 60 min). Concentrations of FAMEs were normalised to volume of sediment.

DNA extraction and multiple displacement amplification of marine subsurfacegenomes

DNA was extracted from 6 g of wet sediment by using ISOIL for Beads Beating kit (Nippon Gene, Tokyo, Japan) according to the modified manufacturer's instructions as follows: sediments were crushed in a liquid nitrogen chamber with FREEZER/MILL 6850 (SPEX SamplePrep LLC, NJ) prior to bead-beating to maximize cell disruption, since very low cell disruption efficiencies were observed when DNA was extracted by previously used techniques without physical treatments[6]. Cell disruption efficiency was monitored by epifluorescence microscopy with SYBR Green I, indicating that approximately 80-90% of total cells were physically disrupted (*Supplementary Figure* 3). However, the physical disruption using FREEZER/MILL was found to be unsuitable for the sandy sediments, likely due to serious damage to the nucleic acids by sand particles while crushing. The derived DNA solution after chemical and enzymatic lysis with SDS and lysozyme was further purified with magnet beads (MagExtractor^{TM}-PCR & Gel Clean up, TOYOBO, Tokyo, Japan). Purified DNA was amplified by multiple displacement amplification (MDA) using phi29 polymerase of the Illustra GenomiPhi V2 Kit (GE Healthcare Bioscience, Tokyo, Japan). Reaction mixtures were prepared in a lamina-flow clean bench to avoid potential contamination of DNA from the air. Genome amplifications including negative controls without samples were monitored by real-time PCR with SYBR Green I (*ref. 7*), and no amplification of negative controls was observed during the amplification step (see *Supplementary Figure 4*). The amplified genomes were further purified with Montage PCR (Millipore, Bedford, MA) by removing random primers and unreacted dNTPs.

Quantitative PCR and slot-blot hybridization analysis

To estimate copy numbers of archaeal and bacterial 16S rRNA genes, quantitative PCR (Q-PCR) was performed with a Power SYBR Green PCR Master Mix by ABI 7300 real-time PCR system according to the manufacturer's instructions (Applied Biosystems, Foster city, CA). For bacterial and archaeal 16S rRNA gene amplifications, the primer sets of Bac27F (*ref. 8*) and EUB338R-I (*ref. 9*), ARC806F (*ref. 10*) and ARC958R (*ref. 11*) were used, respectively. The standard curves for bacterial and archaeal 16S rRNA genes were obtained from genome DNA of *Escherichia coli* and *Pyrococcus horikoshii*, respectively (R^2= 0.998 for Bacteria and 0.995 for Archaea). To minimize potential bias by sequence mismatch for molecular detection, we performed slot-blot hybridization (SBH) using highly conserved probes and purified MDA-genomes blotted on nylon membranes (Roche Diagnostics, Tokyo, Japan). For detection of bacterial and archaeal 16S rRNA genes, EUB338-I, II, III (*ref. 9,12*) and ARC915 (*ref. 13*) probes labelled with digoxigenin were used, respectively. The sequence similarity of the ARC915 probe to 3,978 archaeal 16S rRNA gene sequences including almost all deep marine subsurface clones in our ARB software database showed

that the probe is highly conserved among archaeal 16S rRNA genes: i.e. perfect match: 3,539/3,978 sequences (88.96%), one-base mismatch: 3,904/3,978 sequences (98.14%). The probe match analysis revealed that the sequences with the South African gold mine euryarchaeotic group (SAGMEG) have one or two-base mismatches against ARC915, indicating a potential bias for signal detection by SBH. The membranes were hybridized in Ultrahyb Oligo buffer (Ambion, Austin, TX) at 42 °C and washed twice with 0.2 x SSC (1x SSC: 0.15 M NaCl plus 0.015 M sodium citrate) plus 0.1% SDS at 42 °C and twice with 0.5x SSC containing 0.1% SDS at 46 °C. Signals were detected by immunological and chemiluminescent detection with the chemi-luminescent substrate CSPD® using the DIG luminescent detection kit (Roche Diagnostics, Tokyo, Japan). Genome DNA of *Escherichia coli* and *Pyrococcus horikoshii* were used as the standards for bacterial and archaeal 16S rRNA genes detection, respectively. False-positive detection of bacterial/archaeal 16S rRNA gene by cross-hybridization of archaeal/bacterial probes was checked and no signal was detected on *E. coli* and *P. horikoshii* genome blots by ARC915 and EUB338-I, II, III, probes, respectively. Statistical analysis was conducted with Sigmastat 3.5 (Systat Software, Inc., Richmond, CA). Since Q-PCR, SBH, and previous estimates did not have equal variance, we used the Mann-Whitney rank sum test for comparison of the data sets.

Analysis of total organic carbon (TOC) concentration

Contents of total organic carbon were determined on decalcified sediments after acidification of ~50 mg of freeze dried sediment with 3 N HCl. Residues were analysed on a Leco CS200 analyser.

II. Calculations of inventories of TOC, prokaryotic lipids, and cellular carbon in marine sediments

Horizontal and vertical distribution of TOC, IPLs and biomass-C in marine sediments

Regional provinces based on organic carbon content in surface sediments have been defined by Seiter *et al.*[14] Sediment coverage and area of the provinces were calculated with MATLAB using a grid resolution of 5' from the NGDC sediment thickness database[15] for all grid cells where both TOC and sediment thickness were available (*Supplementary Table* S4). For depth integration, the maximum sediment thickness in each grid cell was limited to account for a hypothetical upper temperature limit under which subsurface life is present in very deep sediments (cf. ref. 16). Assuming a typical geothermal gradient of 30 °C/km and largely sterile conditions at temperatures of 90 to 100 °C, we defined 3000 m deep sediments as the most deeply buried boundary compatible with microbial life. Several provinces were combined to two major environmental types: open-ocean and continental

margin sediments (see *Supplementary Table 4*) with different geological and geochemical parameters (see *Supplementary Table 5*). Down-core concentrations of TOC were calculated on the basis of an empirical diagenetic model (Eq. 1) (*ref. 17*). Equation 3 describes *[TOC](t)* as a function of sediment age *t* and initial age *a,* and is obtained after substitution of Eq. 1 into first-order kinetics of organic carbon degradation (Eq. 2) followed by integration. Initial ages *a* are an expression of the organic matter's initial reactivity and were chosen by reverse fitting of the calculated TOC concentration profile to measured values in the deeper layers. Numerical integration of *[TOC](t)* over time from present to the age of the sediment basement or, at continental margins, the base of the habitable zone, and division by the covered time span (t_{base}) results in the average organic carbon concentration $[TOC]_{av}$ in the environment (Eq. 4). Using the empirical relationship of Eq. 5, the average concentration of IPLs $[IPL]_{av}$ can be calculated from $[TOC]_{av}$. The total amount of IPLs ($m_{IPL,sed}$) is calculated according to Eq. 6 with the volume of the sediment V_{sed} taken from *Supplementary Table 5* and assuming an average sediment density ρ_{sed} of 1.5 g/cm^3. The calculation of biomass-C units ($m_{C,sed}$) is based on Eq. 7 from the amount of IPL/cell ($m_{IPL,cell}$) and carbon/cell ($m_{C,cell}$) and is shown for a cell diameter of 500 nm (Table 1).

$$k(t) = 0.21 \cdot (a + t)^{-0.99} \quad (1)$$

$$\frac{d[TOC]}{dt} = -k(t) \cdot [TOC] \quad (2)$$

$$[TOC](t) = [TOC](0) \cdot e^{21 \cdot \left(\sqrt[100]{a} - \sqrt[100]{a+t}\right)} \quad (3)$$

$$[TOC]_{av} = \int_0^{t_{base}} [TOC](t)\, dt \cdot \frac{1}{t_{base}} \quad (4)$$

$$log[IPL]_{av} = 0.979 \cdot \log[TOC]_{av} + 2.436 \quad (5)$$

$$m_{IPL,sed} = [IPL]_{av} \cdot V_{sed} \cdot \rho_{sed} \quad (6)$$

$$m_{C,sed} = \frac{m_{C,cell}}{m_{IPL,cell}} \cdot m_{IPL,sed} \quad (7)$$

Amounts of IPL and carbon in cells

Published values for cellular amounts of lipids and total carbon vary widely[18-23]. Simon and Azam[23] published well established values for the macromolecular composition of an average spherical marine bacterium in a cell diameter range of 370-910 nm. Their results show that the ratio of cellular carbon to cell membrane lipids does not vary much with cell volume (ratio = 11-15) due to decreasing water content in smaller cells. We transferred their model to archaea by accounting for a lower membrane thickness of 5-6 nm[24] and a lower protein content of 60% (*ref. 25*) and found for spherical archaeal cells with diameters of 400 to 700 nm conversion factors of lipid/cell that are on average only 10% higher than the values

reported for bacteria by Simon and Azam[23]. The amount of IPL/cell ($m_{IPL,cell}$), carbon/cell ($m_{C,cell}$), and the conversion factor cellular carbon/IPL calculated using the power functions[23] for a cell diameter of 500 nm are 1.4 fg, 18 fg and 13.

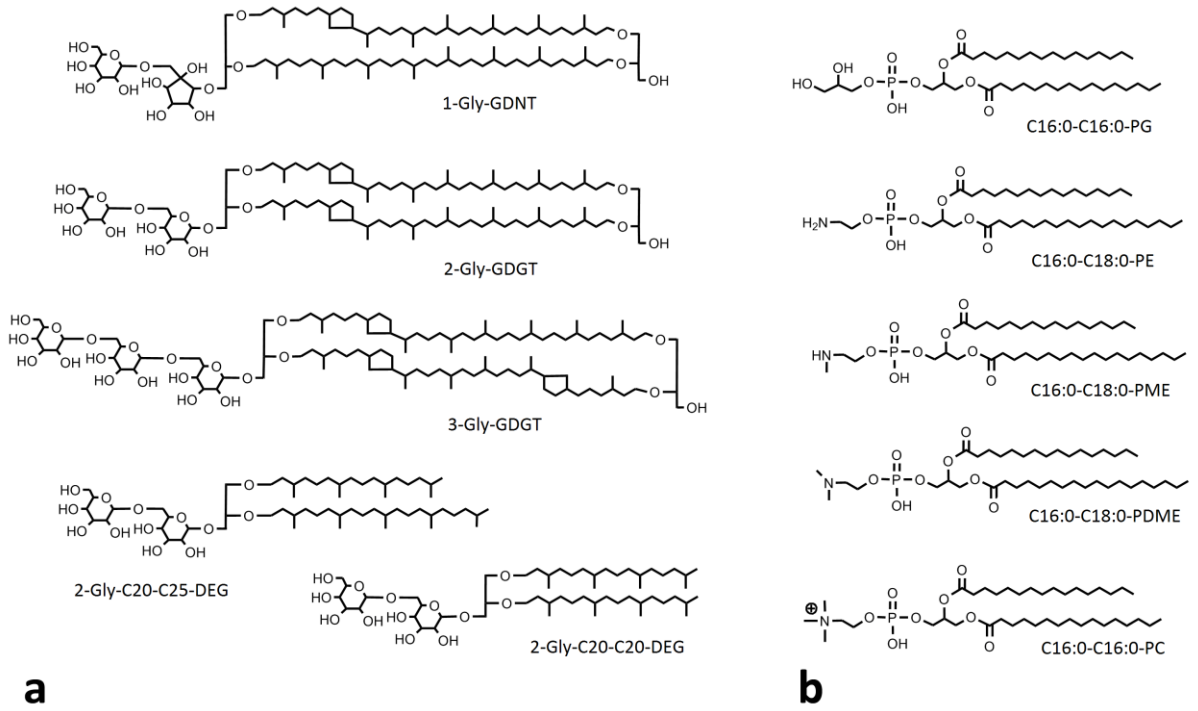

Supplementary Figure 1: Structures of prokaryotic IPLs detected in marine sediments. (A) Archaeal tetraethers with 0-5 rings were found, examples of the core lipid structures with 1-3 rings are shown. **(B)** The most abundant bacterial phospholipid fatty acids were $C_{16:0}$, $C_{16:1}$, $C_{18:0}$, and $C_{18:1}$. Headgroups: 1-Gly: monoglycosyl, 2-Gly: diglycosyl, 3-Gly: triglycosyl, PG: phosphatidylglycerol, PE: phosphatidylethanolamine, PME: phosphatidyl-(N)-methylethanolamine, PDME: phosphatidyl-(N,N)-dimethylethanolamine. Core lipids: GDGT: glycerol dibiphytanyl glycerol tetraether, GDNT: glycerol dibiphytanyl nonitol tetraether, DEG: dietherglycerol.

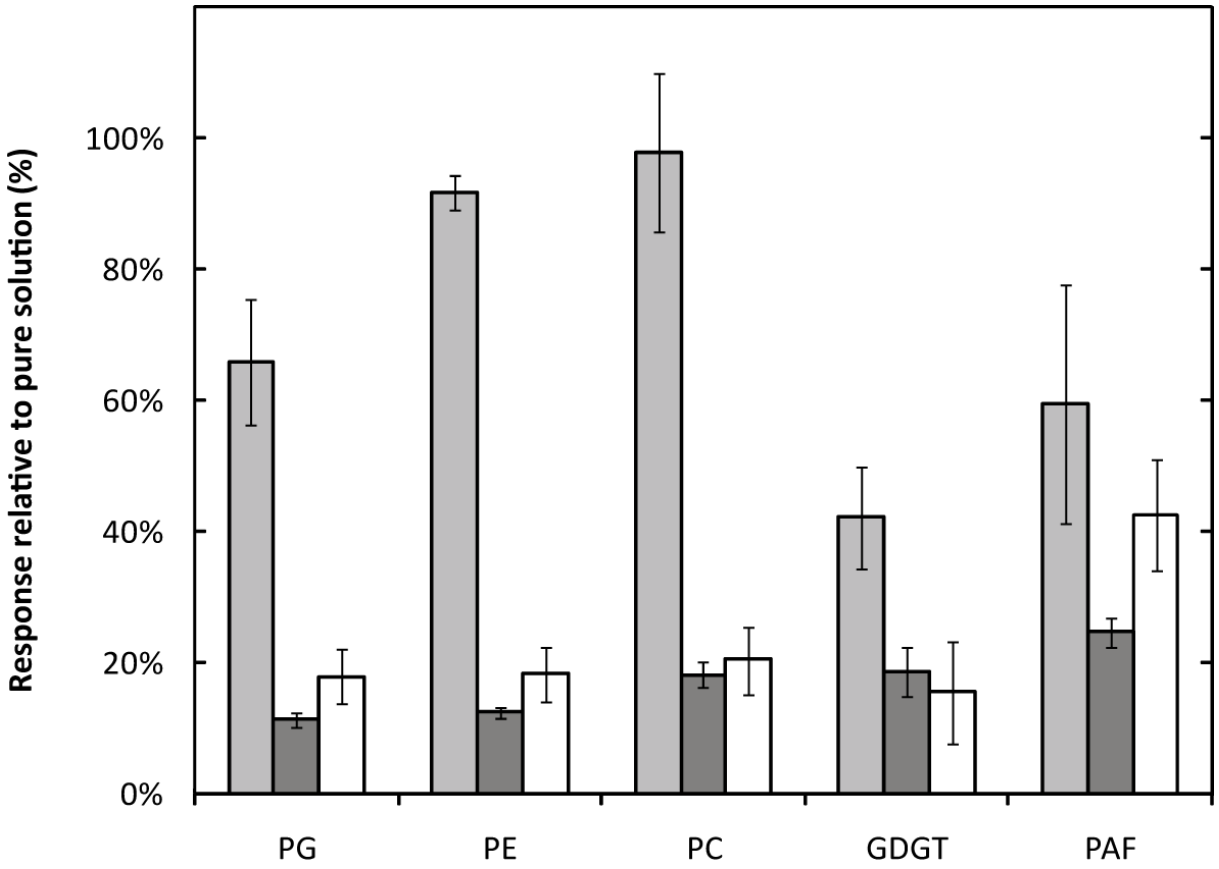

Supplementary Figure 2: Effects of extraction and ion suppression on signal intensity. Samples were spiked with a mixture of five different standards and recovery was calculated relative to directly analysed standard mixture. Two different sediment samples were spiked before extraction: light grey bar: organic-lean sample 1225A-198.1 and dark grey bar: organic-rich sample 1227D-1.15. The white bar shows the result of spiking lipid extract of sample 1227D-21.9 with pure IPLs and direct analysis without extraction. The results demonstrate that there is no systematic discrimination of IPL types during extraction, sample preparation, and mass spectrometric detection. The data clearly show, however, the effect of ion suppression (e.g. *ref. 2*), presumably caused by the extract matrix.

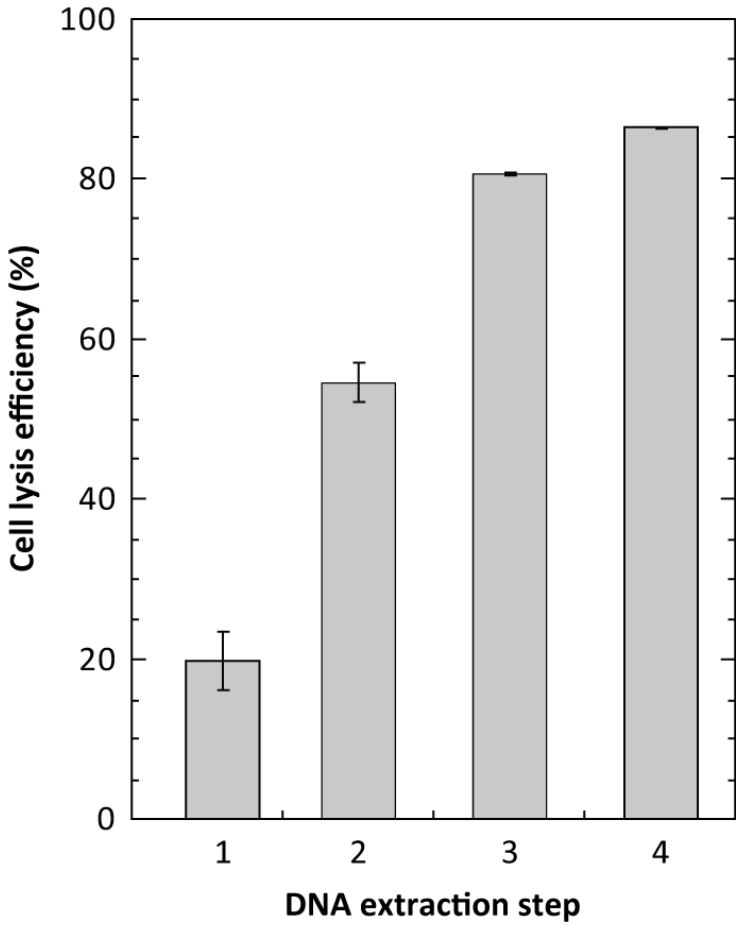

Supplementary Figure 3: **Cell lysis efficiency after chemical, enzymatic, and physical disruption of marine subsurface sediments.** The number of SYBR Green I-stained cells were evaluated under fluorescent microscopy after the following DNA extraction steps: 1) SDS and enzymatic (lysozyme and proteinase K) treatment, 2) beads beating treatment and step (1), 3) freeze mill at beating rate 8 and step (1), and 4) freeze mill at beating rate 15 and step (1). The experiments were carried out sample CK06-06-2T-3. Error bars indicate the standard deviation (n = 5).

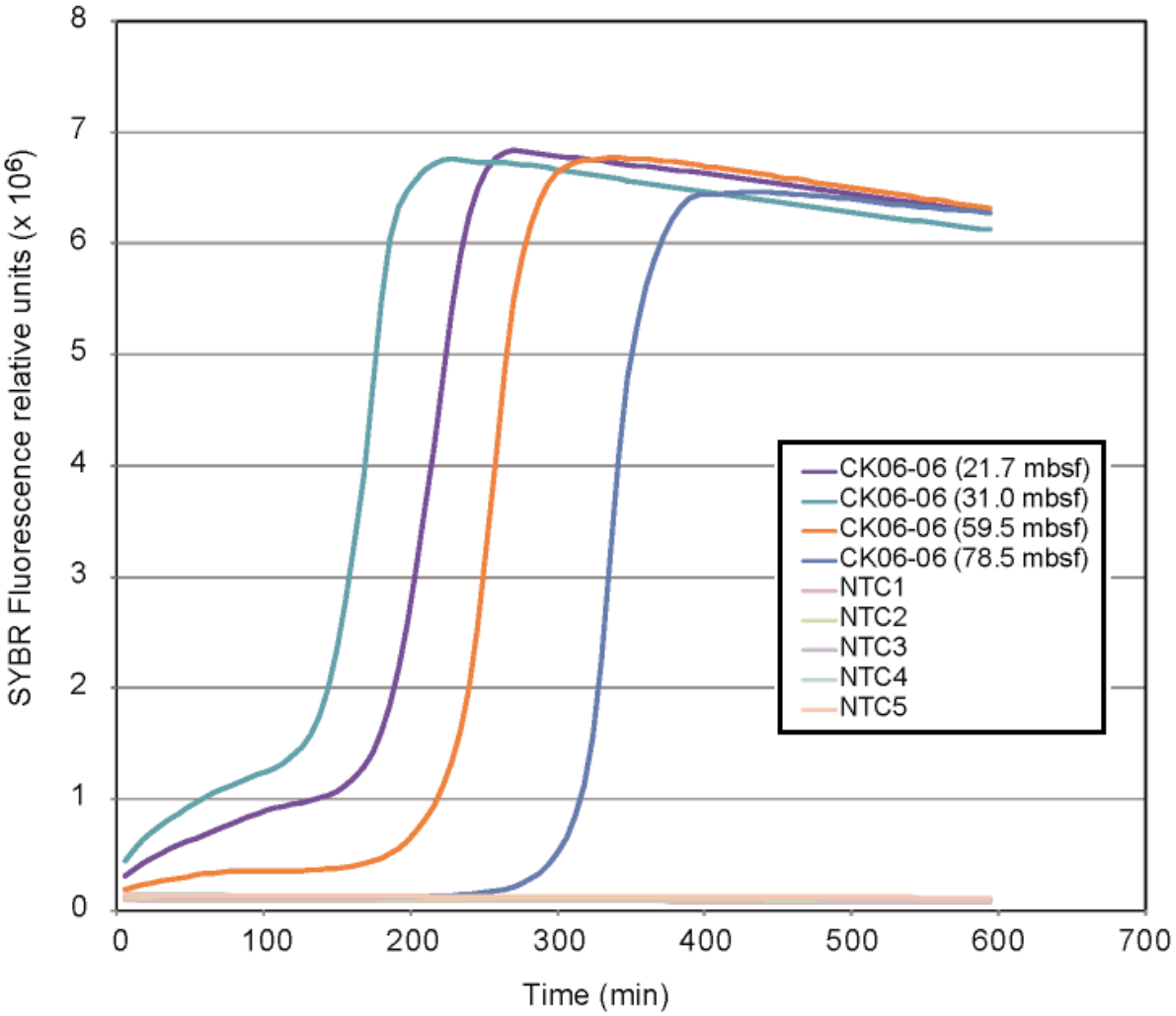

Supplementary Figure 4: **An example of quality control monitoring of multiple displacement amplification evaluated by quantitative real-time PCR with SYBR Green I.** The deep marine subsurface genomes amplified by the reaction of multiple displacement amplification with phi29 polymerase were obtained without amplification of negative control samples. NTC: no-template control.

Supplementary Table 1: Sampling site characteristics and number of samples analysed for IPLs and molecular biological based methods.

Cruise	Station/Site	Position	Water depth (m)	# of samples
SO147	2MC	11°35.0'S 77°3.1'W	86	19
SO147	47MC	9°44.4'S 78°45.1'W	155	13
KY04-11	PC08	33°7.3'N 136°28.8'E	2400	5
TTR15	BS269M	41°57.5'N 41°17.6'E	850	8
ODP leg 201	1226	3°5.7'S 90°49.1'W	3297	7
ODP leg 201	1227	8°59.5'S 90°57.4'W	427	8
ODP leg 201	1229	10°58.6'S 77°57.5'W	152	18
ODP leg 201	1230	9°6.8'S 80°35.0'W	5086	6
ODP leg 204	1250	44°34.1'N 125°9.0'W	796	7
ODP leg 207	1257	9°27.2'N 54°20.5'W	2951	1
ODP leg 207	1258	9°26.0'N 54°44.0'W	3192	1
IODP expedition 301	1301	47°45.2'N 127°45.8'W	2656	4
IODP expedition 311	1326	48°37.6'N 127°3.0'W	1828	2
IODP expedition 311	1327	48°41.9'N 126°51.9'W	1304	3
IODP expedition 311	1329	48°47.3'N 126°40.7'W	946	2
CK06-06	C9001	41°10.6'N 142°12.1'E	1180	21

Supplementary Table 2: Relative abundance of archaeal 16S rRNA genes in sediment cores evaluated by quantitative PCR (Q-PCR) and slot-blot hybridization (SBH).

Station	Depth (mbsf)	Archaeal 16S rRNA gene copy number ratio (%)[a]	
		Q-PCR (N = 3)	SBH (N ≥ 2)
1226E	3.2	50.1 ± 9.1	67.7 ± 38.4
1226B	46.7	25.9 ± 6.2	>12
1227D	0.3	0.08 ± 0.05	82.8 ± 20.4
1227A	16.6	0.06 ± 0.03	11.2 ± 5.11
1227D	42.0	21.7 ± 4.9	40.3 ± 38.0
1227A	75.1	72.6 ± 8.2	59.7 ± 36.8
1230A	0.3	15.1 ± 7.0	49.9 ± 40.9
1230A	6.3	3.1 ± 4.4	8.5 ± 2.2
1230A	29.8	n.d.[c]	43.8 ± 47.9
1230A	73.8	86.9 ± 2.7	66.7 ± 25.3
1230A	209.3	n.d. [c]	17.4 ± 14.1
1301C	2.5	82.7 ± 8.4	56.4 ± 40.8
1301C	51.2	10.1 ± 4.0	46.7 ± 40.8
1301C	90.8	84.3 ± 2.3	36.4 ± 9.8
1301D	122.5	n.d. [c]	n.d. [c]
1301C	259.5	n.d. [c]	53.9 ± 32.4
CK06-06	1.0	39.9 ± 5.7	58.4 ± 32.4
CK06-06	5.2	50.1 ± 1.1	67.2 ± 34.5
CK06-06	8.1	18.1 ± 0.3	58.4 ± 30.3
CK06-06	13.5	97.6 ± 0.8	44.6 ± 30.1
CK06-06	21.7	1.8 ± 0.2	61.2 ± 12.1
CK06-06	31.0	1.5 ± 0.2	52.0 ± 20.9
CK06-06	59.5	0.4 ± 0.2	23.0 (n=1)
CK06-06	78.5	37.6 ± 3.6	4.3 ± 0.2
CK06-06	97.6	6.6 ± 5.5	n.d. [c]
CK06-06	116.6	98.1 ± 0.3	61.8 ± 17.9
CK06-06	134.5	56.5 ± 10.8	54.3 ± 45.7
CK06-06	154.5	0.02 ± 0.03	87.0 (n=1)
CK06-06	171.8	>0.1[b]	>18.9 (n=1) [b]
CK06-06	191.5	14.3 ± 5.2	15.5 ± 16.9
CK06-06	208.3	0.7 ± 0.1	n.d. [c]
CK06-06	216.8	23.2 ± 3.0	30.3 ± 19.0
CK06-06	228.6	88.6 ± 2.6	>11.9 (n=1) [b]
CK06-06	264.9	>97.8[b]	20.2 ± 14.0
CK06-06	346.3	30.0 ± 4.5	60.9 ± 48.2
CK06-06	358.6	34.3 ± 19	46.3 ± 31.0

[a]Archaeal 16S rRNA gene copy number ratio = archaeal 16S rRNA genes / (archaeal + bacterial 16S rRNA genes).
[b]The value indicates the minimum archaeal 16S rRNA ratio based on the detection limit of bacterial 16S rRNA gene copy number when no bacterial signals were detected.
[c]n.d.: not detected

Supplementary Table 3: PLFA and IPL concentrations (in ng mL^{-1}) of selected sediment cores. When no bacterial IPLs were detected, the LOD was assumed as bacterial IPL concentration (see *Supplementary Methods*). The higher PLFA relative to IPL concentrations in sample SO147-2MC might be partially due to inclusion of fatty acids from undefined polar precursors[26] as evidenced by the presence of land-plant derived fatty acids (C_{20}-C_{26}).

	SO147-2MC-0.05	1226B-45.87	1301C-49.90	1229A-185.88
Σ C_{14}-C_{18}	4668	4.8	6.8	1.5
Σ C_{20}-C_{26}	253	0.2	0.8	1.4
Total PLFA	4921	5.0	7.6	2.9
Bacterial IPLs	1036	5.4 (LOD)	125.6 (LOD)	22.7 (LOD)

Supplementary Table 4: Area and TOC contents, and average sediment coverage in marine sediment provinces defined by Seiter *et al.*[14] Provinces of open ocean and continental margin settings were combined to two major environment types and the average TOC content was weighted by area.

Province	Area (10^6 km^2)	Percent of total area	TOC in top 5 cmbsf (%)	Sediment coverage in habitable sediments (m)*
NEPAC	25.98	8.3	0.4	160
NWPAC	18.87	6.0	0.6	347
SEPAC	54.37	17.4	0.5	132
SWPAC	9.27	3.0	0.8	636
TROPAC2	12.32	3.9	0.8	399
TROPAC	30.86	9.9	1.2	197
NOATL	29.35	9.4	0.4	704
SOATL	35.31	11.3	0.4	476
ETROPAT	3.11	1.0	0.7	585
IND	58.87	18.9	0.4	571
EARAB	0.97	0.3	1.2	1343
WARAB	2.20	0.7	1.5	1167
GROE	1.69	0.5	0.7	816
ANT	4.50	1.4	0.3	1522
Σ Open Ocean	**287.68**	**92.1**	**0.56 (weighted by area)**	**416 (weighted by area)**
EUR1	0.295	0.09	0.8	1632
EUR2	1.47	0.47	0.3	1959
NWAMCO	1.77	0.57	1.7	538
NEAMCO	5.92	1.90	0.9	2227
SEAFCO	2.60	0.83	0.5	1834
WAFCO	1.29	0.41	0.6	2402
TANZACO	0.921	0.30	1.0	2155
SOMALICO	0.295	0.09	0.7	1197
GUI	0.353	0.11	1.1	2366
CANAR	0.486	0.16	0.6	2327
GUBRACO	1.58	0.50	0.4	2569
ARGCO	1.53	0.49	0.3	1643
BRAZCO	1.40	0.45	0.5	2194
RIOPLATA	0.813	0.26	0.8	2558
EICO	0.409	0.13	1.0	3000
SWACO	1.92	0.62	1.5	2331
NAMBCO	0.543	0.17	2.7	1618
PERCO	0.542	0.17	4.8	292
CHICO	0.479	0.15	1.5	646
Σ Continental Margin	**24.63**	**7.9**	**0.95 (weighted by area)**	**1952 (weighted by area)**

* maximum sediment thickness was limited to 3000 mbsf during depth integration in individual grid cells to account for an upper temperature limit compatible with life, even if the actual thickness may have been higher.

Supplementary Table 5: Parameters and assumptions for modelling of TOC distribution in marine environment types. Estimates in open ocean and continental margin sediments are based on average sediment coverage of 416 m and 1952 m, respectively. A total area of marine sediments of 360 x 10^6 km^2 (*ref. 27)* was used to calculate sediment volumes. Note that this value is higher than the sum of open ocean and continental margin area in *Supplementary Table 4* of 312 x 10^6 km^2. The relative proportions of 92% open ocean and 8% continental margin are adopted in the area not covered by the NGDC database[15] and/or the study of Seiter *et al.*[14].

	Open Ocean	Continental Margin, habitable zone
Percent of ocean area (%)	92.1	7.9
Sediment coverage (m)	416	1952
Volume of sediment (10^6 km^3)	137.9	55.4
TOC in surface sediment (%)	0.56	0.95
Sedimentation rate (cm kyr^{-1})	0.33	10
Age of sediment base (Myr)	124.9	19.5
Initial Age (yr)	3 x 10^4	1 x 10^4

References

1. Sturt, H. F., Summons, R. E., Smith, K. J., Elvert, M., Hinrichs, K.-U. Intact polar membrane lipids in prokaryotes and sediments deciphered by high-performance liquid chromatography/electrospray ionization multistage mass spectrometry-new biomarkers for biogeochemistry and microbial ecology. *Rap. Comm. Mass. Spec.* **18**, 617-628 (2004).

2. Mallet, C. R., Lu, Z., Mazzeo, J. R. A study of ion suppression effects in electrospray ionization from mobile phase additives and solid-phase extracts. *Rap. Comm. Mass. Spec.* **18**, 49-58 (2004).

3. Mills, C. T., Dias, R. F., Graham, D., Mandernack, K. W. Determination of phospholipid fatty acid structures and stable carbon isotope compositions of deep-sea sediments of the Northwest Pacific, ODP site 1179. *Mar. Chem.* **98**, 197-209 (2006).

4. White, D. C., Bobbie, R. J., King, J. D., Nickels, J. S., Amoe, P. in *Methodology for Biomass Determination and Microbial Activities in Sediments* (eds., Lichtfeld, C. D., Seyfried, P. L.) 87-103 (ASTM STP 673, Philadelphia, 1979).

5. White, D. C., Ringelberg, D. B. in *Techniques in Microbial Ecology* (eds. Burlage, B. S., Atlas, R., Stahl, D.), 255-259 (Oxford University Press: New York, 1998).

6. Inagaki, F. *et al.* Biogeographical distribution and diversity of microbes in methane hydrate-bearing deep marine sediments on the Pacific Ocean Margin. *Proc. Natl. Acad. Sci. USA* **103**, 2815-2820 (2006).

7. Stephanauskas, R., Sieracki, M. E. Matching phylogeny and metabolism in the uncultured marine bacteria, one cell at a time. *Proc. Natl. Acad. Sci. USA* **104**, 9052-9057 (2007).

8. Lane, D. J. in *Nucleic Acid Techniques in Bacterial Systematics* (eds. Stackebrandt, E., Goodfellow, M.) 115-176 (Wiley, New York, 1985).

9. Amann, R. I. *et al.* Combination of 16S rRNA-targeted oligonucleotide probes with flow cytometry for analyzing mixed microbial populations. *Appl. Environ. Microbiol*. **56**, 1919-1925 (1990).

10. Takai, K., Horikoshi, K. Rapid Detection and Quantification of Members of the Archaeal Community by Quantitative PCR Using Fluorogenic Probes. *Appl. Environ. Microbiol*. **66**, 5066-5072 (2000).

11. DeLong, E. F. Archaea in coastal marine environments. *Proc. Natl. Acad. Sci. U.S.A.* **89**, 5685-5689 (1992).

12. Daims, H., Brühl, A., Amann, R., Schleifer, K.-H., Wagner, M. The domain-specific probe EUB338 is insufficient for the detection of all Bacteria: development and evaluation of a more comprehensive probe set. *Syst. Appl. Microbiol.* **22**, 434-444 (1999).

13. Amann, R. I., Krumholz, L., Stahl, D. A. Fluorescent-oligonucleotide probing of whole cells for determinative, phylogenetic, and environmental studies in microbiology. *J. Bacteriol*. **172**, 762-770 (1990).

14. Seiter, K., Hensen, C., Schröter, J., Zabel, M. Organic carbon content in surface sediments—defining regional provinces. *Deep-Sea Res. I* **51**, 2001-2026 (2004).

15. Divins, D. L., NGDC Total Sediment Thickness of the World's Oceans & Marginal Seas, retrieved March 11, 2008, www.ngdc.noaa.gov/mgg/sedthick/sedthick.html.

16. Whitman, W. B., Coleman, D. C., Wiebe, W. J. Prokaryotes: The unseen majority. *Proc. Natl. Acad. Sci. USA* **95**, 6578-6583 (1998).

17. Middelburg, J. J., Vlug, T., van der Nat, F. J. W. A. Organic matter mineralization in marine systems. *Glob. Plan. Change* **8**, 47-58 (1993).

18. Bratbak, G.. Bacterial Biovolume and Biomass Estimations. *Appl. Environ. Microbiol*. **49**, 1488-1493 (1985).

19. Balkwill, D. L., Leach, F. R., Wilson, J. T., McNabb, J. F., White, D. C. Equivalence of Microbial Biomass Measures Based on Membrane Lipid and Cell Wall Components, Adenosine Triphosphate, and Direct Counts in Subsurface Aquifer Sediments. *Microb. Ecol.* **16**, 73-84 (1988).

20. Morita, R. Y. *Bacteria in Oligotrophic Environments* (Chapman & Hall, New York, pp. 529, 1997).

21. Madigan, M. T., Martinko, J. M., Parker, J. *Brock biology of microorganisms, 9th edition.* (Prentice Hall, London, pp. 991, 2000).

22. Summit, M., Peacock, A., Ringelberg, D., White, D. C., Baross, J. A. Phospholipid Fatty Acid-derived Microbial Biomass and Community Dynamics in hot, hydrothermally influenced Sediments from the Middle Valley, Juan de Fuca Ridge. *Proc. ODP Sci. Res.* **169**, doi:10.2973/odp.proc.sr.169.117.2000 (2000).

23. Simon, M., Azam, F. Protein content and protein synthesis rates of planktonic marine bacteria. *Mar. Ecol. Progr. Ser.* **51**, 201-213 (1989).

24. Bakowsky, U., Rothe, U., Antonopoulos, E., Martini, T., Henkel, L., Freisleben, H.-J. (Monomolecular organization of the main tetraether lipid from *Thermoplasma acidophilum* at the water-air interface. *Chem. Phys. Lipids* **105**, 31-42 (2000).

25. DeRosa, M., Gambacorta, A., Gliozzi, A.. Structure, Biosynthesis, and Physicochemical Properties of Archaeabacterial Lipids. *Microbiol. Rev.* **50**, 70-80 (1986).

26. Aries, E., Doumenq, P., Artaud, J., Molinet, J., Bertrand, J. C. Occurrence of fatty acids linked to non-phospholipid compounds in the polar fraction of a marine sedimentary extract from Carteau cove, France. *Org. Geochem.* **32**, 193-197 (2001).

27. Lisitzin, A. P. *Oceanic Sedimentation: Lithology and Geochemistry* (AGU, Washington, DC, 1996).